

Strongly clustered random graphs via triadic closure: An exactly solvable model

Lorenzo Cirigliano,^{1,2} Claudio Castellano,^{3,2} Gareth J. Baxter,⁴ and Gábor Timár⁴

¹*Dipartimento di Fisica Università “Sapienza”, P.le A. Moro, 2, I-00185 Rome, Italy.*

²*Centro Ricerche Enrico Fermi, Piazza del Viminale, 1, I-00184 Rome, Italy*

³*Istituto dei Sistemi Complessi (ISC-CNR), Via dei Taurini 19, I-00185 Rome, Italy*

⁴*Departamento de Física da Universidade de Aveiro & I3N,
Campus Universitário de Santiago, 3810-193 Aveiro, Portugal*

(Dated: February 16, 2024)

Triadic closure, the formation of a connection between two nodes in a network sharing a common neighbor, is considered a fundamental mechanism determining the clustered nature of many real-world topologies. In this work we define a static triadic closure (STC) model for clustered networks, whereby starting from an arbitrary fixed backbone network, each triad is closed independently with a given probability. Assuming a locally treelike backbone we derive exact expressions for the expected number of various small, loopy motifs (triangles, 4-loops, diamonds and 4-cliques) as a function of moments of the backbone degree distribution. In this way we determine how transitivity and its suitably defined generalizations for higher-order motifs depend on the heterogeneity of the original network, revealing the existence of transitions due to the interplay between topologically inequivalent triads in the network. Furthermore, under reasonable assumptions for the moments of the backbone network, we establish approximate relationships between motif densities, which we test in a large dataset of real-world networks. We find a good agreement, indicating that STC is a realistic mechanism for the generation of clustered networks, while remaining simple enough to be amenable to analytical treatment.

I. INTRODUCTION

A network representation is a powerful tool for studying a huge variety of complex systems. Random network models, such as the Erdős-Rényi model [1, 2], the more general configuration model [3–5] and its various extensions [6] have enjoyed considerable popularity due to their amenability to mathematical analysis. These random networks have a locally treelike structure in the infinite size limit, which facilitates the study of branching processes (e.g., percolation, epidemic spreading) and interacting systems (e.g., the Ising model) on top of these substrates [7].

An important feature of many real-world networks is a non-vanishing density of short loops, in particular triangles [8], which is at significant odds with the locally tree-like structure assumption. The propensity of node triads to form triangles is often quantified by the local clustering coefficient or the global transitivity [6]. While the presence of clustering in networks has significant effects on processes such as percolation and epidemics [9–11], both the mean local clustering coefficient and the transitivity tend to zero in the infinite size limit of locally treelike random networks. To account for non-vanishing clustering, i.e., a non-vanishing density of triangles in the infinite size limit, Strauss [12] proposed an exponential random graph model with soft constraints on the number of edges and the number of triangles in the network. One may introduce further constraints to achieve specific network structures [13–16]. Although such models are easily generalizable and rather flexible, their use is impeded by the highly non-trivial phase diagrams that can emerge [17], making it difficult to fit real network structures and to study dynamical models.

The latter problem is circumvented in a model proposed by Newman [18] where each node belongs to a prescribed number of partial cliques (fully connected subgraphs where edges are removed with a certain probability) whose sizes are randomly distributed. Since the building blocks—the partial cliques—only overlap at nodes and not at edges, this model allows for analytical treatment using generating functions to study percolation and related processes. The same approach is used in Refs. [19, 20] where each node is prescribed an edge-degree and a triangle-degree, and nodes are randomly joined together in pairs to form edges (as in the original configuration model) and randomly joined together in groups of three to form triangles. Using only triangles and no higher-order cliques allows for better control over the degree distribution to fit real network data. In an elegant approach Gleeson [21] is able to fit an arbitrary degree distribution and clustering spectrum C_K (the mean clustering coefficient of nodes of degree K) by prescribing an appropriate joint degree and clique size distribution. The modelling approach of randomly connecting cliques or partial cliques may be generalized to randomly connecting arbitrary subgraphs [22]. As long as these subgraphs only overlap at nodes, standard generating function techniques can be used to solve for various network properties such as percolation.

Most real network structures cannot be accurately described by the above random graph models due to the complex overlapping patterns of clustered subgraphs. A very simple and reasonably realistic mechanism—particularly in social networks—that is able to produce high clustering and complex community structure is triadic closure [23]. The idea is that as a network evolves many new links are created between nodes that share a

common neighbour, i.e., by closing triads. Triadic closure is widely considered to be an essential mechanism of structure formation in social networks [24–34]. Most existing models of network formation involving triadic closure are dynamic in nature, that is, the triadic closure mechanism is generally part of a growth or rewiring process. This often makes it difficult to obtain an analytical description and to identify what network features may be directly attributed to triadic closure.

Here we consider a minimal static model of triadic closure, whereby given an existing (backbone) network, a fraction f of existing triads is, on average, closed. In the case of a configuration model backbone this model can be seen as a special case of a more general model recently considered in Ref. [35]. There, triadic closure was applied after creating a network with community structure and degree correlations, using a generalized configuration model. For $f = 1$ static triadic closure implies that all nodes at distance 2 in the backbone become nearest neighbors in the new network. Hence a process involving nearest neighbors on the new clustered network is equivalent to the same process with an extended range of interaction in the original backbone network [36].

The simplicity of this model allows for a detailed analytical description, which is lacking in most of the studies involving triadic closure. By means of the generating function formalism we derive exact results in the case where the original backbone is locally treelike. In particular, network transitivity and densities of other higher-order motifs (such as diamonds or loops of length 4) are expressed in terms of moments of the backbone degree distribution. In this way we uncover the existence of sharp transitions in clustering properties of the model as a function of the heterogeneity of the backbone. The origin of these transitions is traced to the competition between topologically distinct types of subgraphs created by the closure process. A comparison between the model predictions and a large database of networks confirms the plausibility of static triadic closure as a generative mechanism for many real-world structures.

II. MODEL DESCRIPTION

Given a graph $\mathcal{G} = (\mathcal{V}, \mathcal{E})$ with $N = |\mathcal{V}|$ nodes and $E = |\mathcal{E}|$ edges, a triad centered on node j is a sequence of three consecutive nodes $(i, j, k) = (k, j, i)$, i.e. an unoriented path of length two made by the edges $(i, j), (j, k) \in \mathcal{E}$. A triangle $\{i, j, k\}$ is a closed undirected path of length three. Note that for each triangle there are three distinct closed triads. We define the static triadic closure (STC) mechanism as a random process in which each triad becomes a triangle with probability f through the addition of an edge joining its end nodes. Using this STC mechanism, it is possible to build a graph in the following way. We start from a network $\mathcal{G}_0 = (\mathcal{V}, \mathcal{E}_0)$ and we write down all the triads in it. For each triad (i, j, k) , we update the edge set \mathcal{E}_0 by adding to it the edge (i, k)

with probability f . When the triadic closure has been attempted on all the triads in \mathcal{G}_0 , the process ends. The result is a new edge list \mathcal{E}_f with $E_f = |\mathcal{E}_f|$ edges, from which we can define a new network $\mathcal{G}_f = (\mathcal{V}, \mathcal{E}_f)$ with a rich variety of short loops and highly complex structure (see FIG. 1). This algorithm defines an ensemble of random networks, which we will refer to, with a slight abuse of notation, as \mathcal{G}_f .

This algorithm may describe quite different specific mechanisms for triadic closure. One could imagine for instance a triadic closure process in which a node is inclined to be connected with one of its second neighbors with probability ψ , but the triangle is only closed if both nodes agree. This would correspond to a probability of triadic closure $f = \psi^2$. Alternatively, the triad (i, j, k) may be closed if at least one among i and k likes the other, the resulting triadic closure probability is $f = 1 - (1 - \psi)^2$. In both cases, the STC process described as above works with the prescription of using the appropriate probability in place of f .

It is worth remarking that our definition of static triadic closure is fully general: it is possible to generate, using this STC mechanism, random clustered networks starting from any given backbone. In the following sections however, we study the ensemble of graphs \mathcal{G}_f , generated by static triadic closure starting from a random, uncorrelated locally treelike backbone \mathcal{G}_0 , generated using the Uncorrelated Configuration Model [37, 38] with a prescribed degree distribution p_k . We develop the theoretical framework to characterize these STC random graphs, using generating functions to describe the properties of \mathcal{G}_f (see Appendix A 1 for general definitions). Exploiting the local treelikeness of the network \mathcal{G}_0 , it is possible to compute average quantities in \mathcal{G}_f in terms of averages with respect to p_k . Note that in our model there are two distinct and independent sources of randomness: the first is the random nature of the backbone \mathcal{G}_0 , and the second is the random nature of the STC process.

We will denote with lower-case letters quantities which refer to the backbone \mathcal{G}_0 , and with capital letters quantities related to the graph \mathcal{G}_f . In particular $k, r, g_0(z), g_1(z)$ and $K, R, G_0(z), G_1(z)$ denote the degree, excess degree and the corresponding probability generating functions, in the networks \mathcal{G}_0 and \mathcal{G}_f , respectively.

III. THE GENERATING FUNCTION OF THE DEGREE DISTRIBUTION

We begin the study of the network ensemble \mathcal{G}_f by investigating the behavior of its degree distribution $P_K(f)$. For the sake of brevity, we will omit the explicit dependence on f of $P_K(f)$ by writing P_K . Even if we are not able to compute P_K explicitly, it is possible to determine its generating function $G_0(z)$ by expressing it in terms of the generating functions of the degree and of the excess degree distributions in the network \mathcal{G}_0 , $g_0(z)$ and $g_1(z)$, respectively. The result we obtain relies on the fact that

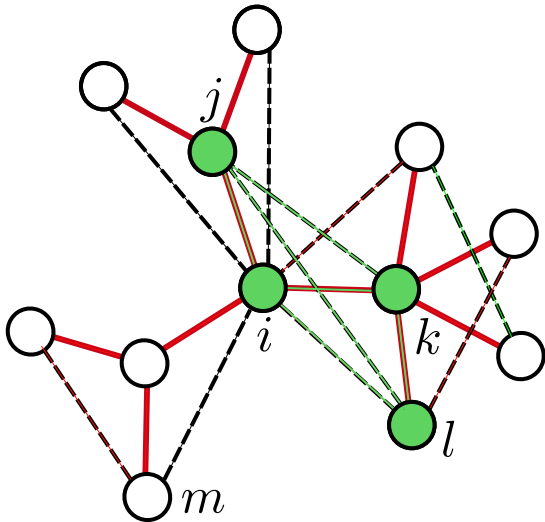


FIG. 1. Pictorial representation of the STC algorithm. The edges of the backbone network \mathcal{G}_0 , a tree with $N = 12$ nodes and $E_0 = 11$ edges, are represented with solid red lines; the dashed black lines represent the edges created by the STC procedure. The result is a network \mathcal{G}_f with $N = 12$ nodes and $E_f = 21$ edges, a variety of short loops and a much more complex structure: many new triads, such as (j, i, l) and (m, i, l) , and many triangles, such as $\{i, k, l\}$, are created, as well as other higher-order motifs, for instance 4-loops – unoriented closed paths of length 4, e.g. $\{i, j, k, l\}$ – and 4-cliques (e.g., the one formed by the nodes shaded in green).

the generating function of a sum of independent random variables is the product of their generating functions.

Consider first the case $f = 1$. K is the random variable representing the degree of a node in \mathcal{G}_1 . Assume that this node has degree k in \mathcal{G}_0 , and label with $i = 1, \dots, k$ its first neighbors. We can write $K = k + \sum_{i=1}^k r_i$, where r_i is the excess degree of first neighbor i . Since the network \mathcal{G}_0 is uncorrelated, the generating function of the variable K , conditioned on having degree k in \mathcal{G}_0 , is given by $[zg_1(z)]^k$. Averaging then over the degree distribution p_k we get $G_0(z) = g_0(zg_1(z))$. This standard argument can be generalized to arbitrary f by considering $K = k + \sum_{i=1}^k n_i$, where n_i are random variables, ranging from 0 to r_i , representing the number of new connections made with second neighbors in the i -th branch. The variables n_i are independent random variables distributed according to binomial distributions $B^{(i)}(n; r_i, f) = \binom{r_i}{n} f^n (1-f)^{r_i-n}$. We can now repeat the argument used for $f = 1$ by simply conditioning not only on k , but also on r_1, \dots, r_k . Hence, for fixed k, r_1, \dots, r_k , we get $z^k \prod_{i=1}^k [(1-f+fz)^{r_i}]$, where $(1-f+fz)^{r_i}$ is the generating function of the binomial distribution $B^{(i)}(n_i, r_i; f)$. Averaging over the excess degree distributions q_{r_1}, \dots, q_{r_k} and over p_k we finally get for the generating function of the degree distribution P_K in \mathcal{G}_f

$$G_0(z) = g_0(zg_1(1-f+fz)). \quad (1)$$

The degree distribution P_K may be computed, at

least in principle, from Eq. (1) by differentiation, since $G_0(z) = \sum P_K z^K$, see Appendix A 2. Unfortunately, this cannot be done explicitly in a closed form for a generic p_k ¹. However, in general it is possible to obtain asymptotic estimates of P_K for large K . For instance, if \mathcal{G}_0 has a power-law (PL) degree distribution $p_k \sim k^{-\gamma}$, the resulting \mathcal{G}_f is a PL network with $P_K \sim K^{-\gamma'}$, with $\gamma' = \gamma - 1$, that is the exponent is decreased by one (see Appendix A 2 a for details).

From the generating function in Eq. (1) we can compute every moment $\langle K^n \rangle$. In particular, the average degree in \mathcal{G}_f is given by

$$\langle K \rangle = G'_0(1) = \langle k \rangle + f \langle k(k-1) \rangle, \quad (2)$$

which simply states that, on average, each node is connected to a fraction f of its second neighbors, reflecting the basic mechanism of static triadic closure. It is important to notice that if \mathcal{G}_0 is a truly sparse graph, that is if $\langle k \rangle = \mathcal{O}(1)$, see [39], the STC procedure creates a truly sparse graph \mathcal{G}_f only if $\langle k^2 \rangle = \mathcal{O}(1)$. In some cases, such as PL with $\gamma < 3$, $\langle k^2 \rangle = \mathcal{O}(N^\alpha)$ for some $0 < \alpha < 1$, and hence $\langle K \rangle = \mathcal{O}(N^\alpha)$. Models defined on such networks with a slowly diverging mean degree may exhibit a qualitatively different critical behavior from the truly sparse case, see for instance [36].

It is useful to define the factorial moments μ_n by

$$\mu_n = \langle k(k-1) \dots (k-n+1) \rangle = g_0^{(n)}(1) \quad (3)$$

(see Appendix A 3 for more details).

IV. CLUSTERING

Armed with the generating function for the final degree distribution, we may study the various properties of the new network. Since it is the principal motivation for the model, we begin by studying clustering properties, the presence of triangles in the network.

We first focus on the global clustering coefficient of the network \mathcal{G}_f , also called transitivity, which is the ratio between three times the total number of triangles to the number of triads in the network. We then discuss the behavior of the mean local clustering coefficient which is the ratio between the number of triangles connected to and the number of triads centered on a particular node, averaged over all nodes.

A. Transitivity

The global clustering coefficient is defined as [38]

$$T = \frac{3N_\Delta}{N_\wedge}, \quad (4)$$

¹ It is possible to obtain an exact expression for P_K if the backbone is a random regular network.

where N_Δ and N_\wedge denote the average total number of triangles and triads, respectively².

1. General results

Exploiting the local treelikeness of the underlying backbone network, it is possible to exactly compute the transitivity of the network \mathcal{G}_f .

The average number of triads in \mathcal{G}_f can be evaluated easily. Take a node of degree K in \mathcal{G}_f . To form a triad, we can pick one among K of its neighbors, and then one among $K - 1$ remaining other neighbors: hence such a node is the center of $K(K - 1)/2$ different triads. Averaging over the degree distribution P_K we get

$$\begin{aligned} N_\wedge &= N \left\langle \binom{K}{2} \right\rangle = \frac{N}{2} G_0''(1) \\ &= \frac{N}{2} [g_0''(1)(1 + f g_1'(1))^2 + 2f g_0''(1) + f^2 g_0'''(1)] \\ &= \frac{N}{2} [\mu_2(1 + f\mu_2/\mu_1)^2 + 2f\mu_2 + f^2\mu_3], \end{aligned} \quad (5)$$

where we express the average over P_K in terms of the derivatives of the generating function $G_0(z)$ and we use Eq. (1).

To compute the average total number of triangles we can proceed in the following way. Consider a node i of degree k in \mathcal{G}_0 , and consider its neighborhood. We evaluate the average number of triangles that are created in its neighborhood, and then average over the degree distribution p_k . With the help of FIG. 2, it is easy to see that triangles in the neighborhood of node i can be of only two types: either they are made by joining two neighbors of node i via the triadic closure process, with probability f (type A); or they are made by joining together three neighbors of node i , with probability f^3 (type B). Since both these types are defined with reference to the node i , one may verify that the triangles will only be counted once. The average number of triangles of type A is $f k(k - 1)/2$, while the average number of triangles of type B is $f^3 k(k - 1)(k - 2)/3!$, hence summing these two contributions together and averaging over p_k we obtain

$$N_\Delta = \frac{Nf}{6} [3\mu_2 + f^2\mu_3]. \quad (6)$$

Substituting into Eq. (4) we get

$$T = \frac{f(3\mu_2 + f^2\mu_3)}{\mu_2(1 + f\mu_2/\mu_1)^2 + 2f\mu_2 + f^2\mu_3}. \quad (7)$$

For Erdős-Rényi (ER) backbones, since $\mu_n = c^n$, Eq. (7) reduces to

$$T = \frac{3f + f^3c}{1 + 2f(1 + c) + f^2c(1 + c)}. \quad (8)$$

² The factor 3 takes into account the fact that in each triangle there are three distinct triads.

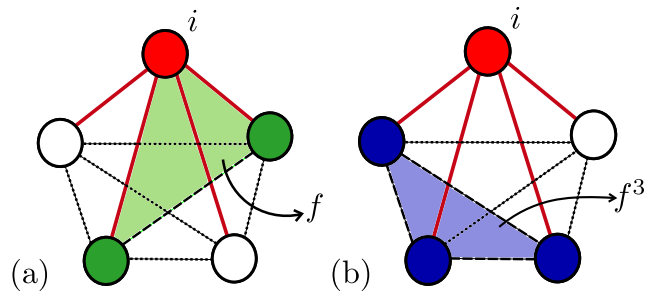


FIG. 2. A visualization of the triangle counting. Consider node i of degree $k = 4$, coloured in red, and its neighbors. The edges in \mathcal{G}_0 are represented with solid red lines, while the black dotted lines are the edges that may be created by the STC mechanism and hence may appear in \mathcal{G}_f . We can distinguish between triangles of type A – shaded in green in (a) – made of two already existing edges and one new edge, and triangles of type B – shaded blue in (b) – made of three new edges. The total number of potential A-triangles is $\binom{4}{2} = 6$, i.e. the number of edges in the 4-clique composed of i 's neighbors, and each one of them is created with probability f . Over many STC realizations, there are $6f$ of them on average. The total number of potential B-triangles is $\binom{4}{3} = 4$, i.e., the number of triangles in the 4-clique composed of i 's neighbors. Each one of them appears with probability f^3 , hence on average there are $4f^3$ of them. The average number of triangles for a node of degree $k = 4$ is then $6f + 4f^3$. Repeating this argument for all nodes we obtain Eq. (6). Note that in this way each triangle is counted exactly once.

In FIG. 3 we compare Eq. (8) with numerical simulations of \mathcal{G}_f networks created from an ER backbone, for different values of the original mean degree c and of the closing probability f . It is worth noting the non-monotonic behavior of $T(f)$ for large, fixed c : for $c > c^* = 5.7531\dots$, $T(f)$ admits a maximum and a minimum in the interval $[0, 1]$. This implies that from the same backbone with $c > c^*$, we can create two graphs \mathcal{G}_{f_1} and \mathcal{G}_{f_2} having the same transitivity and $f_1 \neq f_2$.

2. The case of power-law backbones

The case of \mathcal{G}_f generated from power-law (PL) degree distributed backbones \mathcal{G}_0 with $p_k \sim k^{-\gamma}$ is of particular interest. We assume that $k \in [k_{\min}, k_c(N)]$, and that the maximum degree grows as a power of N whose value depends on the exponent γ : $k_c(N) \sim N^{\omega(\gamma)} \rightarrow \infty$ as $N \rightarrow \infty$ [37], with $0 < \omega \leq 1/2$ for $2 < \gamma \leq 3$ and $\omega = 1/(\gamma - 1)$ for $\gamma > 3$. Some moments of a power-law distribution diverge in the infinite-size limit, depending on the value of γ (see Appendix B). This implies that, for some values of γ , N_Δ and N_\wedge may grow faster than linearly in N ³. A careful analysis of Eq. (7) can be

³ Of course, $3N_\Delta \leq N_\wedge$ always.

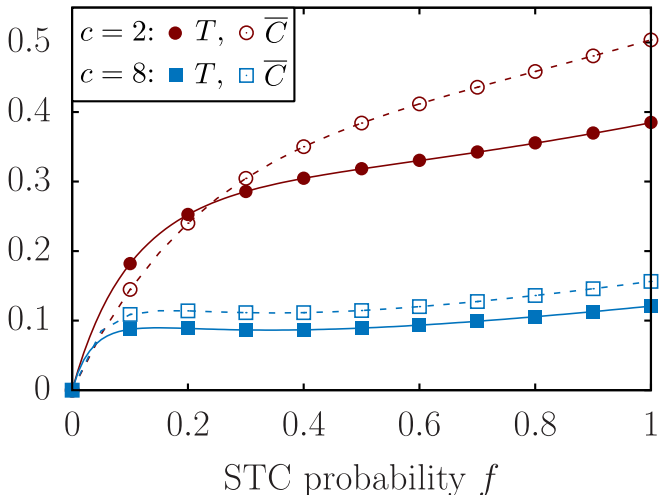


FIG. 3. Transitivity T (filled symbols) and mean local clustering coefficient \bar{C} (empty symbols) as a function of f in networks \mathcal{G}_f generated from ER backbones with mean degree $c = 2$ (circles), $c = 8$ (squares) and size $N = 10^6$, averaged over 10 realizations of the STC procedure. The continuous lines correspond to the exact expression for the transitivity in Eq. (8) and they are in perfect agreement with simulation results. Dashed lines are not an analytic solution but simply a guide to the eye.

carried out, using the fact that, when the factorial moments diverge, they are dominated by the leading term, hence $\mu_n \sim \langle k^n \rangle$, so that they can be used to stand in for the moments of the degree distribution. Expressions for them are given in Appendix B. For $\gamma > 4$ none of the terms appearing in Eq. (7) diverge in the limit of infinite network size, and the transitivity is a nonlinear function of f and γ which can be computed using the expressions for μ_n in Eqs.(B7)-(B10). More interesting is the case $\gamma \leq 4$, in which some of the terms in Eq. (7) diverge. We get, in the limit $k_c \rightarrow \infty$,

$$T \simeq \begin{cases} 0 & \text{for } 2 < \gamma < 5/2, \\ \frac{f}{1+c(k_{\min})} & \text{for } \gamma = 5/2, \\ f & \text{for } 5/2 < \gamma \leq 4, \end{cases} \quad (9)$$

where $c(k_{\min})$ is a constant, depending only on k_{\min} , given by the ratio of the diverging moments $\mu_2^3/(\mu_3\mu_1^2)$ evaluated at $\gamma = 5/2$. Within the continuous degree approximation (see Appendix B) $c(k_{\min}) = 3k_{\min}$. Eq. (9) reveals a discontinuity in T at $\gamma = 5/2$, as observed in FIG. 4(a). This discontinuous behavior occurs because, while the number of triangles is asymptotically $\langle k^3 \rangle$, the number of triads is asymptotically proportional to $\langle k^2 \rangle^3 + a\langle k^3 \rangle$, where a is a constant. At $\gamma = 5/2$ the dominant term in the number of triads changes, causing the abrupt transition observed in T .

To understand this dual behavior of the number of triads, we identify five classes of topologically different triads in \mathcal{G}_f . Denoting with i_0 the center node of the triad (i_1, i_0, i_2) , with the help of FIG. 5 we can classify

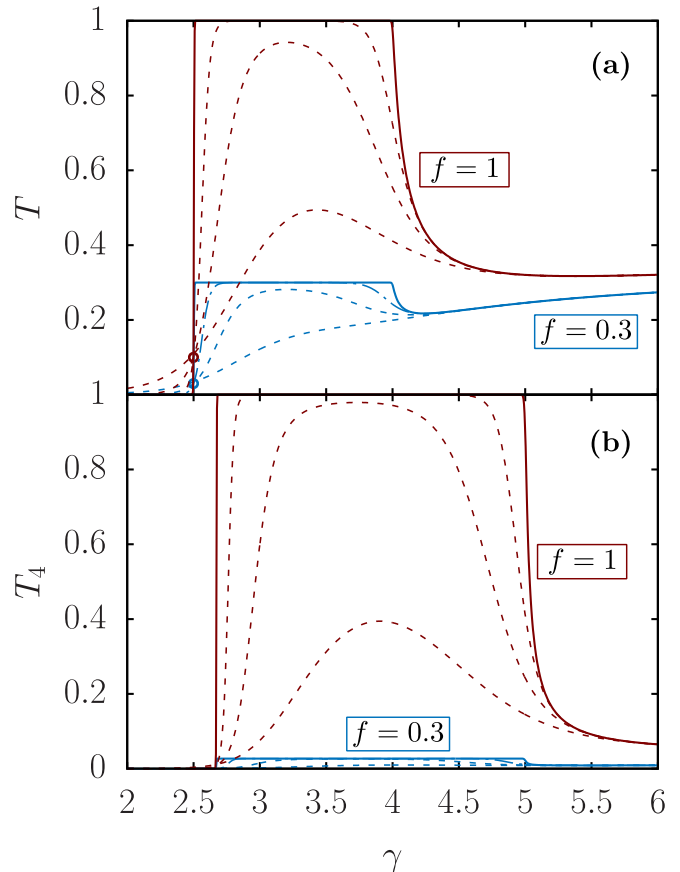


FIG. 4. Analytical expressions for (a) transitivity, Eq. (7), and (b) 4-transitivity, Eq. (22) for $n = 4$, in STC networks with a PL backbone, as a function of γ , for two different values of the STC probability f . These curves are obtained evaluating Eqs. (7), (22) within a continuous degree approximation, with $k_{\min} = 3$. Continuous lines correspond to the infinite-size limit $k_c \rightarrow \infty$, dashed lines are for $k_c = 10^3, 10^5, 10^{10}$. Circles in panel (a) correspond to the values for $\gamma = 5/2$ given in Eq. (9).

triads as follows.

- I. Triads in which both i_1 and i_2 were i_0 's neighbors in \mathcal{G}_0 , such as $(1, 0, 2)$ in FIG. 5. By construction, a fraction f of these triads is closed on average.
- II. Triads in which i_1 and i_2 were i_0 's first and second neighbors, respectively, but i_1 and i_2 were not neighbors in \mathcal{G}_0 , e.g. $(2, 0, 3)$ in FIG. 5. These triads are always open in \mathcal{G}_f .
- III. Triads in which both i_1 and i_2 were i_0 's second neighbors in \mathcal{G}_0 , but i_1 and i_2 did not have a common neighbor, such as $(3, 0, 6)$ in FIG. 5. These triads are always open in \mathcal{G}_f .
- IV. Triads in which i_1 was i_0 's neighbor and i_2 was i_1 's neighbor in \mathcal{G}_0 , e.g. $(1, 0, 3)$ in FIG. 5. Note that these triads are always closed.

V. Triads in which both i_1 and i_2 were i_0 's second neighbors in \mathcal{G}_0 , and i_1 and i_2 had a common neighbor, such as (5, 0, 6) in FIG. 5. A fraction f of these triads is closed on average.

We refer to triads in classes (I,II,III) as *interbranch triads*, since they all involve nodes within different branches in \mathcal{G}_0 . Conversely, triads in classes (IV,V) involve nodes within the same branch in \mathcal{G}_0 , therefore we call them *inbranch triads*. It is worth noting that terms corresponding explicitly to these five cases appear in Eq. (5) after expanding the term $(1+f\mu_2/\mu_1)^2$. For $2 < \gamma \leq 3$, the leading contributions are both of order $\mathcal{O}(f^2)$ and come from triads in classes III and V. Indeed, triads from class III contribute to the denominator of T with the term

$$\frac{N_{\Delta}^{(\text{III})}}{N} = \frac{\mu_2}{2}(f\mu_2/\mu_1)^2 \sim \langle k^2 \rangle^3 \sim k_c^{3(3-\gamma)},$$

where the first μ_2 is the average number of ways of choosing two distinct branches emanating from a random node i , and the factor $(\mu_2/\mu_1)^2$ is the average number of i 's second neighbors in each of such branches. Triads from class V contribute to the denominator of T with

$$\frac{N_{\Delta}^{(\text{V})}}{N} = f^2 \frac{\mu_3}{2} = \frac{f^2}{2} \mu_1 (\mu_3/\mu_1) \sim \langle k^3 \rangle \sim k_c^{4-\gamma},$$

where the factor μ_1 is the average number of branches emanating from a random node i , and μ_3/μ_1 is the average number of pairs of i 's second neighbors along each branch. Note that while triads in class V are closed with probability f – indeed they also appear in the numerator of Eq. (7) – triads in class III are always open. Hence if $N_{\Delta}^{(\text{III})} \ll N_{\Delta}^{(\text{V})}$, that is for $\gamma > 5/2$, the dominant term $N_{\Delta}^{(\text{V})}$ appears both in the numerator and the denominator of Eq. (7), yielding $T = f$. For $\gamma < 5/2$ instead, the dominant contribution comes from open triads $N_{\Delta}^{(\text{III})}$, and this gives $T = 0$. Then the abrupt change in T occurs when $N_{\Delta}^{(\text{III})}$ scales as $N_{\Delta}^{(\text{V})}$, that is at $\gamma = 5/2$. For $3 < \gamma \leq 4$, $N_{\Delta}^{(\text{III})}$ is finite and the dominant contribution coming from $N_{\Delta}^{(\text{V})}$ appears both at the numerator and at the denominator of Eq. (7), yielding $T = f$. In other words, while for $5/2 < \gamma \leq 4$ the STC mechanism creates (almost) only closed intrabranched triads, for $\gamma < 5/2$ it produces infinitely many more open interbranch triads than closed triads.

In finite systems, one observes a slow convergence to the asymptotic results as the system size increases, as illustrated in FIG. 4.

B. Local clustering coefficient

The local clustering coefficient $C_i = n_i^{\Delta}/n_i^{\wedge}$ is the ratio between the number of triangles connected to and the number of triads centered on node i . The mean local clustering $\overline{C} = 1/N \sum_i C_i$ is another global measure

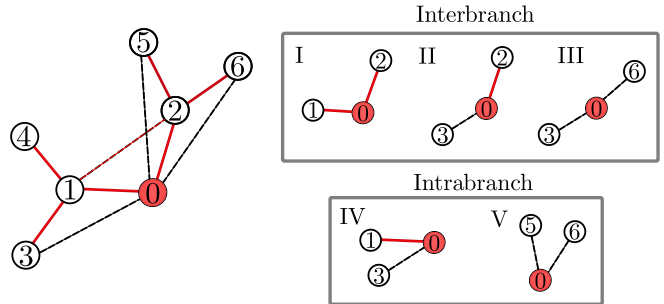


FIG. 5. The five classes of topologically different triads. On the left, a pictorial visualization of an STC process, solid red lines represent the edges in \mathcal{G}_0 and dashed black lines represent the edges created by the STC procedure. On the right, five topologically different intrabranched and interbranch triads centered on node 0.

of the network structure. While in general T and \overline{C} do not coincide, they both tend to zero with the system size in locally treelike random network models [40, 41]. We measure numerically \overline{C} in STC networks obtained from ER backbones, and we compare it with transitivity in FIG. 3. Despite some quantitative difference, the two quantities exhibit the same qualitative behavior in this case. A different scenario occurs in STC networks obtained from PL backbones. We measure numerically \overline{C} for various values of γ and report the results in FIG. 6. It turns out that the mean clustering coefficient does not exhibit the transitions occurring for transitivity in the large- N limit. Instead \overline{C} changes smoothly with γ and also displays much smaller finite size effects. We can get some physical intuition of this qualitative difference between \overline{C} and T by expressing T as a weighted average of the local clustering coefficient C_i [38]

$$T = \frac{3 \times \frac{1}{3} \sum_i n_i^{\Delta}}{\sum_i n_i^{\wedge}} = \frac{\sum_i n_i^{\Delta} C_i}{\sum_i n_i^{\wedge}}. \quad (10)$$

For PL backbones with $\gamma < 4$ both the numerator and the denominator in Eq. (10) diverge, as we already observed in Eq. (9). For $\gamma < 5/2$, however, the divergence of the numerator is tamed by the factor C_i , and the result is a vanishing transitivity.

V. HIGHER-ORDER MOTIFS

The complex structure of \mathcal{G}_f is not limited to a large number of triangles. Higher-order motifs, such as overlapping triangles, loops and cliques, are also naturally created by the STC mechanism. In this Section, by exploiting the treelike structure of \mathcal{G}_0 we derive exact expressions for the number of some higher-order motifs in \mathcal{G}_f .

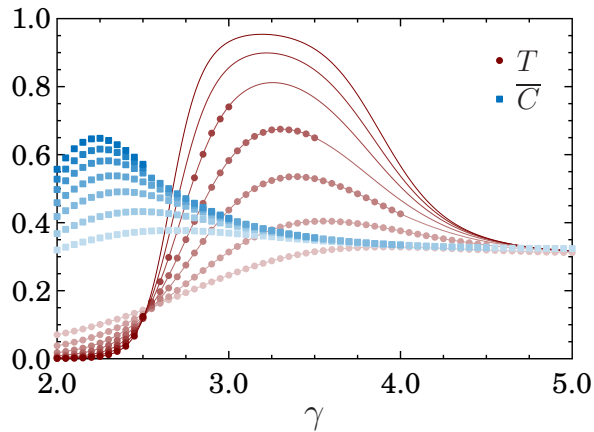


FIG. 6. Transitivity T and mean local clustering coefficient \bar{C} as a function of γ for PL backbones, for different values of k_c , with $f = 1$ and $k_{\min} = 3$. Values of k_c : 100, 300, 1000, 3000, 10000, 30000, 100000. Darker colors correspond to bigger values of k_c . The solid red lines are the exact transitivity values, obtained by numerically evaluating Eq. (7). Markers correspond to simulation results. In order to correctly sample a PL degree distribution, for a given k_c , the number of nodes in the sample must fulfil $N > k_c^{\gamma-1}$. This criterion makes simulations involving high k_c and γ values computationally infeasible. For $\gamma \rightarrow \infty$ the PL backbone network converges to a random regular network of degree k_{\min} . In this limit, since all degrees are the same, both T and \bar{C} are easily evaluated when $f = 1$: $\lim_{\gamma \rightarrow \infty} T = \lim_{\gamma \rightarrow \infty} \bar{C} = 1/k_{\min}$. This limit is already clearly observed for $\gamma \approx 5$.

A. Diamonds and 4-loops

A ubiquitous feature of real social networks is not only their high clustering, but that triangles tend to overlap, significantly altering the dynamics in various types of processes occurring on these networks. The frequency of triangle overlaps both in the STC model and in real-world networks may be measured in various ways. Here we focus on diamonds (two triangles that share a link, that we call the “center” of the motif) and 4-loops (loops of length 4).

1. Average number of diamonds

The easiest way to compute the expected number of diamonds in \mathcal{G}_f , denoted by N_{\square} , is to write

$$N_{\square} = N_{\square}^{(\text{old})} + N_{\square}^{(\text{new})},$$

where $N_{\square}^{(\text{old})}$ and $N_{\square}^{(\text{new})}$ are the number of diamonds centered on old links, i.e. links that are in \mathcal{E}_0 , and on new links, i.e. links that are in $\mathcal{E}_f \setminus \mathcal{E}_0$, respectively. Consider an old edge (as (1, 2) in FIG. 7) with end nodes i and j . Denoting by $n_{i \rightarrow \partial j}$ the number of new links created on average by the STC mechanism between node i and j 's

neighbors, we can distinguish three topologically different diamonds centered on the old link (i, j) (see FIG. 7(a)):

- I. the ones in which we take two among j 's neighbors which have become also i 's neighbors. There are $n_{i \rightarrow \partial j}(n_{i \rightarrow \partial j} - 1)/2$ of them;
- II. the ones in which we take two among i 's neighbors which have become also j 's neighbors. There are $n_{j \rightarrow \partial i}(n_{j \rightarrow \partial i} - 1)/2$ of them;
- III. the ones in which we consider one neighbor of node i and one neighbor of node j . There are $n_{i \rightarrow \partial j}n_{j \rightarrow \partial i}$ of them.

Summing these contributions and averaging over p_k we get

$$N_{\square}^{(\text{old})} = \frac{N \langle k \rangle}{4} \langle \eta_{ij}(\eta_{ij} - 1) \rangle \quad (11)$$

where $\eta_{ij} = n_{i \rightarrow \partial j} + n_{j \rightarrow \partial i}$. Using the fact that $n_{i \rightarrow \partial j}$ and $n_{j \rightarrow \partial i}$ are i.i.d. random variables whose probability generating function is given by $g_1(1 - f + fz)$ (see Sec. III), it follows that the generating function of the probability distribution of the variables η_{ij} is $H(z) = [g_1(1 - f + fz)]^2$. Hence we have

$$N_{\square}^{(\text{old})} = \frac{N \langle k \rangle}{4} H''(1) = \frac{N f^2}{2} [\mu_3 + \mu_2^2/\mu_1]. \quad (12)$$

Now consider a node of degree k in \mathcal{G}_0 , and a new edge (a, b) created among its neighbors. A diamond centered on this edge can be formed only because of the creation of new links among the other $(k - 2)$ neighbors of the node, since nodes a and b are second neighbors in the original network. There are on average $f k(k - 1)/2$ new links such as (a, b). This link can be the center either of a diamond with 2 old links and 2 new links on the perimeter, or can be the center of a diamond with 4 new links on the perimeter (see FIG. 7(b)). First we consider the diamonds with two old links on the perimeter. Fixed the link (a, b), there are $k - 2$ ways of choosing the third node, and hence we have $f^3 k(k - 1)(k - 2)/2$ distinct motifs. In the other case, we can pick the two other nodes to complete the diamond by choosing among the remaining $(k - 2)(k - 3)$ nodes, and we can do this in $(k - 2)(k - 3)/2$ distinct ways. The total number of such motifs is $f^5 k(k - 1)(k - 2)(k - 3)/4$. Averaging over p_k we get

$$N_{\square}^{(\text{new})} = N \left[f^3 \frac{\mu_3}{2} + f^5 \frac{\mu_4}{4} \right]. \quad (13)$$

Summing up we finally have

$$N_{\square} = \frac{N f^2}{4} [2\mu_2^2/\mu_1 + 2(1 + f)\mu_3 + f^3\mu_4]. \quad (14)$$

2. Average number of 4-loops

To compute the average number of 4-loops, a simple observation is crucial: any 4-loop must contain either zero or two old links, by construction. The average number of 4-loops with two old edges, denoted by $N_{\square}^{(2)}$, is the same as the number of diamonds centered on old links given in Eq. (12), see FIG. 7. The number of 4-loops with zero old links, denoted $N_{\square}^{(0)}$, is instead simply given by (see FIG. 7(c))

$$N_{\square}^{(0)} = \frac{Nf^4\mu_4}{8}, \quad (15)$$

since we have $k(k-1)(k-2)(k-3)$ ways of picking 4 nodes among the neighbors of a random node of original degree k , and in a loop the order in which we choose the nodes matters: we have 4 possible ways of starting the loop, and 2 possible choices of orientation, which gives the factor $1/8$. Putting these two contributions together we get

$$N_{\square} = \frac{Nf^2}{8} [4\mu_3 + 4\mu_2^2/\mu_1 + f^2\mu_4]. \quad (16)$$

3. 4-loops made of overlapping triangles

It is useful to define the quantity⁴

$$R_{\square} = \frac{N_{\square}}{2N_{\square}}, \quad (17)$$

which provides a measure of how likely 4-loops are to be made of overlapping triangles (diamonds) in \mathcal{G}_f . In an arbitrary network, any diamond corresponds to exactly one 4-loop. Also, any 4-loop corresponds to at most two diamonds. Therefore, for any network $R_{\square} \in [0, 1]$. From Eqs. (14),(16) we get

$$R_{\square} = \frac{[2\mu_2^2/\mu_1 + 2(1+f)\mu_3 + f^3\mu_4]}{[4\mu_3 + 4\mu_2^2/\mu_1 + f^2\mu_4]}. \quad (18)$$

From this expression, it follows that for PL networks $R_{\square} \rightarrow f$ as $k_c \rightarrow \infty$ for $2 < \gamma \leq 5$, since the most divergent term μ_4 is the same in the numerator and the denominator, while for $\gamma > 5$, the ratio R_{\square} is, in the same limit, a nontrivial function of f always different from 0 and 1. In this case (in fact, for any backbone where the first four moments of the degree distribution are finite) we have $\lim_{f \rightarrow 0} R_{\square} = 1/2$. This means that for small but finite f , each 4-loop corresponds to exactly one diamond.

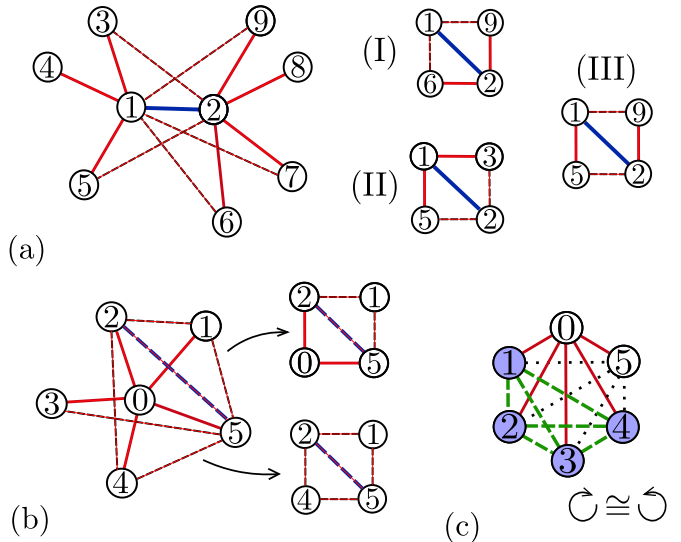


FIG. 7. A pictorial visualization of diamond and 4-loop counting. Solid lines correspond to links in \mathcal{G}_0 , dashed lines are the links created by the STC mechanism. (a) diamonds centered on the old link (1, 2) (thicker line in blue) for a specific realization of the STC process. On the right, we identify the three types of topologically different motifs. Here there are $3 \cdot 2/2 = 3$ motifs of type (I), $2/2 = 1$ motif of type (II) and $3 \cdot 2 = 6$ motifs of type (III). Summing these three terms and averaging gives Eq. (11). Note that these motifs always correspond to 4-loops, and no other 4-loops with 2 old links on the perimeter are possible, since \mathcal{G}_0 is locally treelike. (b) diamonds centered on new links for a particular realization of the STC process. We consider the neighborhood of node 0 of degree $k_0 = 5$. Arrows indicate two topologically different diamonds centered on the new links (2, 5) (thicker line in blue). (c) Counting the 4-loops with no old links on the perimeter. Here we consider the neighborhood of node 0 with degree $k_0 = 5$, and the 4-loop created among nodes 1, 2, 3, 4 (shaded in blue). There are 4 distinct ways of choosing the starting node, and a factor $1/2$ arises by the symmetry under inversion. Hence taking into account these symmetries we have $4 \cdot 3 \cdot 2/(4 \cdot 2) = 3$ distinct 4-loops (dashed green lines): $\{1, 2, 3, 4\}$, $\{1, 3, 2, 4\}$, $\{1, 3, 4, 2\}$. Considering that each 4-loop has a probability f^4 of being created, averaging over the whole network we get Eq. (15).

B. Cliques, stars and generalized transitivity

In this section, we present a generalization of the transitivity to higher-order motifs. It is defined by

$$T_n = \frac{nN_{\mathbb{K}_n}}{N_{S_{n-1}}}, \quad (19)$$

where $N_{\mathbb{K}_n}$ and $N_{S_{n-1}}$ denote the number of n -cliques – complete subgraphs with n nodes, \mathbb{K}_n – and the number of $(n-1)$ -stars – subgraphs made by one node and $n-1$ leaves, S_{n-1} – in \mathcal{G}_f , respectively. The multiplicative factor n takes into account the fact that for each complete subgraph \mathbb{K}_n there are n distinct stars S_{n-1} . Note that for $n = 2$ Eq. (19) trivially reduces to $T_2 = 1$, while for

⁴ Only for $f > 0$, since for $f = 0$ both the numerator and the denominator are zero.

$n = 3$ we recover the standard transitivity $T_3 = T$ as in Eq. (4). It is straightforward to derive expressions for $N_{\mathbb{K}_n}$ and $N_{S_{n-1}}$ for arbitrary n , following the same line of argument which led us to Eqs. (5),(6). We get

$$N_{S_{n-1}} = N \left\langle \binom{K}{n-1} \right\rangle = \frac{N}{(n-1)!} G_0^{(n-1)}(1), \quad (20)$$

where $G_0^{(n-1)}(1)$ can be computed using Eq. (C3), and (it is sufficient to generalize FIG. 2 for arbitrary n -cliques)

$$\begin{aligned} N_{\mathbb{K}_n} &= N \left[f^{\frac{(n-1)(n-2)}{2}} \left\langle \binom{k}{n-1} \right\rangle + f^{\frac{n(n-1)}{2}} \left\langle \binom{k}{n} \right\rangle \right] \\ &= \frac{N f^{(n-1)(n-2)/2}}{n!} [n\mu_{n-1} + f^{n-1}\mu_n]. \end{aligned} \quad (21)$$

Substituting into Eq. (19) we get

$$T_n = \frac{f^{(n-1)(n-2)/2}(n\mu_{n-1} + f^{n-1}\mu_n)}{M_{n-1}}, \quad (22)$$

where we set $M_n = \langle K(K-1)\dots(K-n+1) \rangle$. The study of T_n for PL backbones reveals an interesting feature. It is possible to show that, for $k_c \gg k_{\min}$ (see Appendix C)

$$M_{n-1} \sim \begin{cases} k_c^{n-\gamma+(n-1)(3-\gamma)} & \text{for } 2 < \gamma < \gamma_{(n)}^*, \\ k_c^{n+1-\gamma} & \text{for } \gamma_{(n)}^* < \gamma < n+1, \\ 1 & \text{for } n+1 < \gamma, \end{cases} \quad (23)$$

where

$$\gamma_{(n)}^* = 3 - \frac{1}{n-1}. \quad (24)$$

Hence for $\gamma > n+1$ none of the terms in T_n diverges. For $\gamma \leq n+1$, since $N_{\mathbb{K}_n} \sim N k_c^{n+1-\gamma}$, we get

$$T_n \simeq \begin{cases} 0 & \text{for } 2 < \gamma < \gamma_{(n)}^*, \\ \frac{f^{(n-1)(n-2)/2}}{1+c_n(k_{\min})} & \text{for } \gamma = \gamma_{(n)}^*, \\ f^{(n-1)(n-2)/2} & \text{for } \gamma_{(n)}^* < \gamma \leq n+1, \end{cases} \quad (25)$$

where $c_n(k_{\min})$ is a constant depending only on n and k_{\min} . Eq. (25) shows that the generalized transitivity T_n exhibits a discontinuity at $\gamma_{(n)}^*$, in perfect analogy with the behavior of T discussed in Sec. IV A 2. FIG. 4(b) illustrates the discontinuous transition of T_n with $n = 4$. The competition between two kinds of topologically distinct $(n-1)$ -stars – those created between one node and its second neighbors in a given branch and those created between one node and the second neighbors reached along $n-1$ different branches, with the former dominating over the latter for $\gamma > \gamma_{(n)}^*$ – is responsible for the observed discontinuous behavior of T_n .

VI. MOTIFS IN REAL-WORLD NETWORKS

It is important to compare this model's predictions with corresponding quantities measured in real networks.

The structure of the assumed original backbone network of a given real-world network cannot be easily inferred. Instead we can derive some approximate relations (given some reasonable assumptions) between measurable quantities, which are expected to hold for any network generated via the static triadic closure process starting from a locally treelike backbone.

Our first assumption involves only the moments of the “final” network observed degree distribution: $\langle K^m \rangle \gg \langle K^{m-1} \rangle$ for $m \geq 2$. This condition holds in the large size limit for PL networks with exponent $\gamma' < 3$, which is where most observed values in real networks tend to fall. Our second assumption involves the moments of the backbone with those of the observed network: $\langle K^m \rangle \approx f^m \langle k^{m+1} \rangle$. This relation holds exactly in the large size limit when the backbone network is PL with $\gamma > 3$ (see Appendix C). This would correspond to $\gamma' > 2$ in the final observed network (see Sec. III), which, again, is where most real-world networks tend to be.

These assumptions are exact in the large size limit when the backbone network is PL with $\gamma \in [3, 4]$, which corresponds to the range $\gamma' \in [2, 3]$ in the final observed network. While real networks have a very complicated structure, are finite, and are certainly not exactly power-law degree-distributed, we believe that our assumptions may still be expected to be reasonable in many networks with heavy-tailed degree distribution. Note that we do not make any assumptions about the particular shape of the backbone degree distribution, i.e., we do not fit any parameters, such as the degree distribution exponent γ .

Under the above assumptions, using the results of Sections IV and V we can write the following simple approximate expressions for the densities of the various motifs considered in Sec. V,

$$n_{\square} \equiv \frac{N_{\square}}{N} \approx \frac{T \langle K^3 \rangle}{8}, \quad (26)$$

$$n_{\square} \equiv \frac{N_{\square}}{N} \approx \frac{T^2 \langle K^3 \rangle}{4}, \quad (27)$$

$$n_{\boxtimes} \equiv \frac{N_{\boxtimes}}{N} \approx \frac{T^3 \langle K^3 \rangle}{24}, \quad (28)$$

that is, the densities of motifs involving four nodes depend only on the transitivity and the third moment of the degree distribution. Using Eq. (28) we can write the following simple approximate expression for the 4-transitivity,

$$T_4 = \frac{4N_{\boxtimes}}{N_{S_3}} \approx T^3. \quad (29)$$

Note that the approximate forms in Eqs. (26), (27), (28) and (29) were derived using some simple assumptions related with the moments of the degree distributions and did not require any fitting of parameters. Thus they constitute universal relations. We tested these relations in a dataset of 95 real-world networks of various nature (see

Ref. [42]⁵ for details on the dataset). The results are shown in FIG. 8. Despite the extremely simple form of the approximate expressions, they appear to be in reasonable agreement with empirical results for most networks.

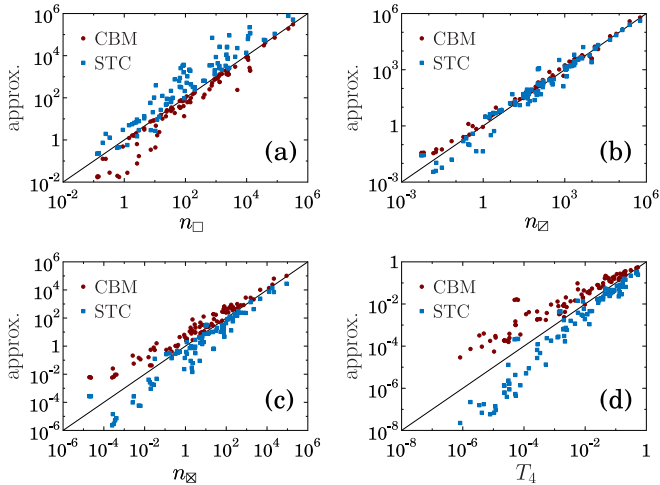


FIG. 8. The CBM and STC [Eqs. (26-29)] approximations to the (a) density of 4-loops, (b) density of diamonds, (c) density of 4-cliques, and (d) 4-transitivity, as a function of the actual observed values in a varied dataset of 95 real-world networks. In each panel one marker corresponds to one network.

To further assess the validity of the approximate relations derived from the STC model, a comparison with other models of clustered networks is worthwhile. As mentioned in Sec. I, most existing mathematically tractable models of clustered networks involve a random linking of triangles, complete or partial cliques, or other higher-order motifs. Unfortunately most of these models are not easily fitted to real networks, therefore the range of applicability of relations derived within them is not easily established. One clique-based model where this can actually be done in a particularly elegant manner is due to Gleeson [21]. In this model each node belongs to exactly one clique and any number of external links. Importantly, the joint degree and clique size distribution in this model can be exactly fitted to a given network degree distribution and clustering spectrum C_K . For this reason we chose this model, as a representative of clique-based models, to compare our results to, and we will refer to it as *clique-based model* (CBM). In the CBM the quantities n_{\square} , n_{\diamond} , n_{\boxtimes} and T_4 are easily calculated as functions of the moments of the clique-size distribution, which we fitted to the clustering spectra of the 95 real networks considered. The resulting values are presented in FIG. 8. While both the CBM and STC models produce reasonable approximations⁶, there are interesting differences to be considered.

The differences are due to the fact that the CBM and STC models realize, in a sense, two opposite extreme approaches to producing clustered networks. In the CBM, triangles only exist within complete cliques, and this leads to an overestimation of denser motifs, e.g., 4-cliques and an underestimation of sparser motifs such as 4-loops. On the other hand, in the STC model triangles are produced in a more homogeneous, diffuse manner, resulting in the opposite trend: an underestimation of 4-cliques and an overestimation of 4-loops⁷.

A quantity that sharply highlights the difference between the two models is the normalized ratio R_{\boxtimes} of the number of diamonds to 4-loops [see Eq. (17)]. This quantity always has the trivial value $R_{\boxtimes}^{(\text{CBM})} = 1$ in clique-based network models (made of complete cliques), since one 4-loop corresponds to exactly two diamond motifs in this case. This property of clique-based models, demonstrating the extreme concentration of triangles, is clearly at odds with structures observed in real-world network data. In the STC model, using the assumptions outlined at the beginning of this section, this ratio is simply given by the transitivity, $R_{\boxtimes}^{(\text{STC})} \approx T$. FIG. 9 shows that, for the 95 real-world networks considered, the STC model provides reasonable approximations for R_{\boxtimes} in some cases, although in general underestimates the true values.

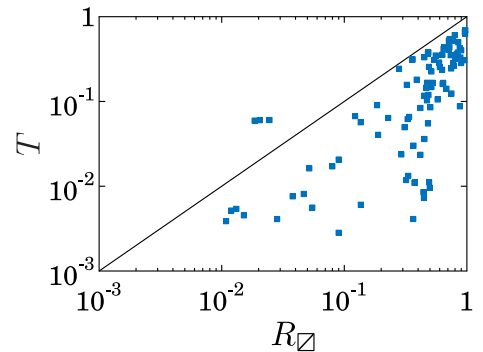


FIG. 9. The STC approximation ($\approx T$) to the ratio R_{\boxtimes} [see Eq. (17)], as a function of the actual observed value in a varied dataset of 95 real-world networks. One marker corresponds to one network.

These results suggest that more realistic versions of the STC model may be achieved by adopting a non-homogeneous triadic closure mechanism, where the probability of closing a triad depends on local structural properties. An obvious candidate for such local properties to consider would be node degrees: in general one may pre-

⁵ Some of the largest networks in the original database could not be considered as they exceeded our computational resources.

⁶ It is important to remark that the relations derived from the STC

model are universal and did not require any parameter fitting, while the values for the CBM were obtained by fitting the entire degree distribution and clustering spectrum of a real network.

⁷ Another comparison of real world clustering statistics with Gleeson's model and a different kind of random model, using rewiring and also matching the clustering spectrum, was made in Ref. [43].

scribe an arbitrary function $f(k_1, k_2, k_3)$ for the probability of closing a triad of degrees k_1, k_2, k_3 . This would allow for substantial control over the extent to which triangles overlap to form loopy motifs, and would allow for the modelling of various forms of the clustering spectrum C_K .

VII. DISCUSSION AND CONCLUSIONS

In this paper we studied in detail a static model of random clustered networks based on the mechanism of triadic closure. In particular, we start from a “backbone” network of arbitrary degree distribution and, with a given probability f , we close each of the existing triads. In the case where the backbone is an uncorrelated locally tree-like network, due to its simplicity this model allows for exact analytical results regarding clustering properties of the network.

We found an exact expression for transitivity and we showed anomalous behavior of this quantity in large power-law degree-distributed networks; transitivity is equal to 0 in the infinite size limit for degree distribution exponent $\gamma < 5/2$ and transitivity is equal to f for $5/2 < \gamma < 4$.

This sharp transition is reminiscent of another transition occurring for this value of γ . Indeed, the largest eigenvalue of the adjacency matrix (spectral radius) of power-law networks is $\langle k^2 \rangle / \langle k \rangle \sim k_c^{3-\gamma}$ for $\gamma < 5/2$, while it is $k_c^{1/2}$ for $\gamma > 5/2$ [44, 45]. In that case, the transition is related to the localization of the principal eigenvector of the adjacency matrix, either on the K-core of maximum index or on the largest hub and its nearest neighbors [46]. The identification of the role of interbranch and intrabranched triads in the behavior of transitivity provides a complementary and clarifying view. In networks with $\gamma < 5/2$ a large max K-core is present. In such structures the neighbors of nodes with large degree have many neighbors in their turn. This is reflected by the dominance of interbranch processes in the STC model. For $\gamma > 5/2$ instead, the spectral radius is determined by the largest hub and its direct neighbors, which tend to have a small number of neighbors. Correspondingly the transitivity is dominated by the formation of connections among the hub’s neighbors (intrabranched processes).

To quantify the density of higher order cliques we defined a generalized transitivity T_n as the number of n -cliques in the network relative to their maximum possible number (in perfect analogy to standard transitivity). We found an exact expression for the general T_n and showed that this quantity undergoes a discontinuous transition—analogue to the standard case—at $\gamma_{(n)}^* = 3 - 1/(n - 1)$.

Using generating functions and simple combinatorial considerations we found exact expressions for the densities of various small loopy motifs, as functions of the first few moments of the backbone degree distribution. Importantly, all motifs in the STC model are produced by triangles (closed triads) overlapping in various ways, i.e.,

all emerging small-scale structures are purely induced by the random triadic closure mechanism. This circumstance makes the STC model a useful tool to evaluate the plausibility of the triadic closure mechanism in real-world networks. With some reasonable assumptions about the moments of the degree distribution, we derived some universal relations between the densities of small loopy motifs. Specifically, we were able to express the density of various motifs involving four nodes as a function of transitivity and of the third moment of the degree distribution. We showed that these remarkably simple, universal relations, hold up reasonably well in real-world networks.

Many interesting research avenues, opened by this work, deserve further investigation. First, while this paper focuses on global quantities, it would be important to understand in detail also the behavior of local quantities, such as the degree distribution P_K , the local clustering coefficient C_i , and degree-degree correlations. Second, the generalization of the approach used in [36] for percolation on the STC model with $f = 1$ can provide insight into the behavior of percolation and other processes on networks with strong clustering and many short loops. Finally, the STC procedure can be generalized to build hypergraphs, by considering not only the edges created by the STC mechanism but also the triangles, as well as higher-order motifs, as hyperedges. The motif counting analysis developed in this work can be straightforwardly generalized in this case, providing a nontrivial, yet exactly solvable, model for triadic interaction.

Appendix A: Probability generating functions

1. General definitions

Given a discrete probability distribution f_k , the associated generating function is defined as

$$g(z) = \langle z^k \rangle = \sum_k f_k z^k, \quad (\text{A1})$$

where the sum is intended over the whole range of k values for which f_k is defined. In case of a continuous variable with probability density $f(k)$, we define

$$g(z) = \int dk f(k) z^k. \quad (\text{A2})$$

For our purposes, we consider the degree distribution $p_k = N_k/N$, where N_k is the number of nodes with degree k , with $k \in [k_{\min}, k_c(N)]$, where $k_c(N)$ diverges in the infinite-size limit. We denote by $g_0(z)$ the degree distribution generating function. Another useful distribution to consider is q_r , where the random variable r is the so-called excess degree, i.e., the degree of a node at which we arrive following a randomly chosen edge excluding the edge we arrived from. We can express q_r in terms of p_k . Indeed, we can compute the probability of reaching a node of excess degree r , and hence degree $r + 1$,

following a randomly chosen edge. This is simply given by

$$q_r = \frac{(r+1)N_{r+1}}{\sum_r (r+1)N_{r+1}} = \frac{(r+1)p_{r+1}}{\langle k \rangle}. \quad (\text{A3})$$

This expression allows us to express the generating function $g_1(z) = \sum_r q_r z^r$ in terms of g_0 by

$$g_1(z) = \frac{g'_0(z)}{g'_0(1)}. \quad (\text{A4})$$

2. Analytic and asymptotic methods

Given a generating function $g_0(z)$ it is possible to obtain the coefficients p_k , i.e. the probability distribution p_k , by differentiation [6]

$$p_k = \frac{1}{k!} \frac{d^k}{dz^k} g_0(z) \Big|_{z=0} = \frac{1}{2\pi i} \oint_{\mathcal{C}} dz \frac{g_0(z)}{z^{k+1}}, \quad (\text{A5})$$

where \mathcal{C} is an arbitrary path around the origin in the complex z plane. It is quite rare that this procedure can be carried out explicitly for any k . Nevertheless, complex analysis developed many tools to estimate the asymptotics of the coefficients p_k for large k . For instance, if $g_0(z)$ is analytic, then $g_1(z)$ is also analytic and the composition of analytic functions is analytic too. Hence we know for sure that P_K cannot exhibit a power-law tail [47]. If instead the generating function $g_0(z)$ exhibits a singular behavior for $z \rightarrow 1^-$, it is possible to know the asymptotic behavior of the coefficients of the series expansion around $z = 0$, that is the asymptotics of p_k for large k . In particular, we recall the following result (Theorem 1 and its corollaries in [48]): if $f(z) = \sum_n f_n z^n$ is analytical in the unitary circle in the complex plane excluding $z_0 = 1$, and as $z \rightarrow 1$ in this domain, $f(z) \sim c(1-z)^\alpha$ for α real, then for noninteger α we have

$$f_n \sim \frac{c}{\Gamma(-\alpha)} n^{-\alpha-1}, \quad n \rightarrow \infty. \quad (\text{A6})$$

Hence for a singular $g_0(z)$ it is sufficient to expand around 1, using $\epsilon = 1 - z$ as a small parameter, to get the asymptotic form of p_k .

a. The degree distribution of G_f with PL backbone

Using Eq. (A6) and the expansions for the generating functions of a PL degree distribution

$$\begin{aligned} g_0(1-\epsilon) &\simeq 1 - \langle k \rangle \epsilon + \frac{1}{2} \langle k \rangle B \epsilon^2 + C(\gamma-1) \epsilon^{\gamma-1}, \\ g_1(1-\epsilon) &\simeq 1 - B \epsilon + \frac{1}{2} D \epsilon^2 + C(\gamma-2) \epsilon^{\gamma-2}, \end{aligned}$$

where B , D and C are constants depending on γ and k_{\min} ⁸, from Eq. (1) we get

$$G_0(1-\epsilon) \simeq 1 - [\langle k \rangle + f \langle k \rangle B] \epsilon + \langle k \rangle C (\gamma-2) (f \epsilon)^{\gamma-2}. \quad (\text{A7})$$

From Eq. (A6) we get for $K \rightarrow \infty$

$$P_K \sim \frac{\langle k \rangle C (\gamma-2) f^{\gamma-2}}{\Gamma(2-\gamma)} K^{-(\gamma-1)},$$

from which we conclude that the STC procedure on PL backbones with exponent γ produces (asymptotically) PL networks with exponent $\gamma' = \gamma - 1$.

3. Computing averages using generating functions

Generating functions are useful tools because they contain information about the whole probability distribution in a very compact way [47]⁹. Indeed, taking the derivatives of the generating functions we can evaluate averages. It is easy to see that, defining the n -th factorial moment [49] $\mu_n = \langle k(k-1) \dots (k-n+1) \rangle$

$$\mu_n = \left[\left(\frac{d}{dz} \right)^n g_0(z) \right] \Big|_{z=1}, \quad (\text{A8})$$

$$\langle k^n \rangle = \left[\left(z \frac{d}{dz} \right)^n g_0(z) \right] \Big|_{z=1}, \quad (\text{A9})$$

where we used the fact that $g_0(z) = \langle z^k \rangle = \langle e^{k \ln z} \rangle$ and $z d/dz = d/d(\ln z)$.

It is possible to express $\langle k^n \rangle$ as a linear combination of μ_j for $j \leq n$ using the relation [50]

$$\left(z \frac{d}{dz} \right)^n f(z) = \sum_{j=1}^n \left\{ \begin{matrix} n \\ j \end{matrix} \right\} z^j \left(\frac{d}{dz} \right)^j f(z), \quad (\text{A10})$$

where $\left\{ \begin{matrix} n \\ j \end{matrix} \right\}$ denote the Stirling numbers of the second kind, whose expression is given by [47, 50]

$$\left\{ \begin{matrix} n \\ j \end{matrix} \right\} = \sum_{i=1}^j \frac{(-1)^{j-i} i^n}{i!(j-i)!}.$$

Evaluating Eq. (A10) for $f(z) = g_0(z)$ at $z = 1$ we get

$$\langle k^n \rangle = \sum_{j=1}^n \left\{ \begin{matrix} n \\ j \end{matrix} \right\} \mu_j. \quad (\text{A11})$$

⁸ See Appendix G in [36] for their explicit values and, in particular, their signs depending on the value of γ .

⁹ From [47], "A generating function is a clothesline on which we hang up a sequence of numbers [probabilities] for display."

Remarkably, Eq. (A11) states for ER networks, for which $\mu_j = c^j$, that

$$\langle k^n \rangle = \sum_{j=1}^n \left\{ \begin{matrix} n \\ j \end{matrix} \right\} c^j,$$

that is $\langle k^n \rangle$ is a power series in c whose coefficients are the Stirling numbers of the second kind.

On the other hand, it is possible to express μ_n in terms of $\langle k^n \rangle$ for $j \leq n$ using the Stirling numbers of the first kind $\left[\begin{matrix} n \\ j \end{matrix} \right]$ which are defined by the relation [51]

$$\prod_{j=0}^{n-1} (x-j) = \sum_{j=1}^n (-1)^{n-j} \left[\begin{matrix} n \\ j \end{matrix} \right] x^j. \quad (\text{A12})$$

Evaluating Eq. (A12) for $x = k$ and averaging over p_k we get

$$\mu_n = \sum_{j=1}^n (-1)^{n-j} \left[\begin{matrix} n \\ j \end{matrix} \right] \langle k^j \rangle. \quad (\text{A13})$$

Appendix B: Moments of power-law distributions

Given a power law probability distribution $p_k \sim k^{-\gamma}$ with $k \in [k_{\min}, k_c]$, we have

$$p_k = \frac{k^{-\gamma}}{\zeta(\gamma, k_{\min}) - \zeta(\gamma, k_c)} \simeq \frac{k^{-\gamma}}{\zeta(\gamma, k_{\min})}, \quad (\text{B1})$$

where $\zeta(\gamma, x) = \sum_{k \geq x} k^{-\gamma}$ is the Hurwitz zeta function [52]. The moments of the distribution are given by

$$\langle k^n \rangle = \frac{\zeta(\gamma - n, k_{\min}) - \zeta(\gamma - n, k_c)}{\zeta(\gamma, k_{\min}) - \zeta(\gamma, k_c)}. \quad (\text{B2})$$

To make computations less cumbersome, we can adopt the continuous-degree approximation, in which the degree is assumed to be a continuous variable. Note that the larger the value of k_{\min} , the better this approximation works. We have

$$p_k = \frac{(\gamma - 1) k_{\min}^{\gamma-1}}{\left[1 - \left(\frac{k_{\min}}{k_c} \right)^{\gamma-1} \right]} k^{-\gamma} \simeq (\gamma - 1) k_{\min}^{\gamma-1} k^{-\gamma}, \quad (\text{B3})$$

$$\langle k \rangle = \frac{\gamma - 1}{\gamma - 2} k_{\min} \left[1 - \left(\frac{k_{\min}}{k_c} \right)^{\gamma-2} \right] \simeq \frac{\gamma - 1}{\gamma - 2} k_{\min}, \quad (\text{B4})$$

for $\gamma > 2$ and $k_c \gg k_{\min}$, which is the case we consider in this paper. For higher order moments of the distribution, the result depends on the value of γ , since the n -th moment may diverge. We have, for $k_c \gg k_{\min}$

$$\langle k^n \rangle = \frac{(\gamma - 1) k_{\min}^{\gamma-1}}{\gamma - n + 1} \left[k_{\min}^{n-(\gamma-1)} - k_c^{n-(\gamma-1)} \right] \quad (\text{B5})$$

$$\underset{k_c \gg k_{\min}}{\simeq} \begin{cases} \frac{\gamma-1}{\gamma-1-n} k_{\min}^n & \text{if } n < \gamma - 1, \\ \frac{\gamma-1}{n+1-\gamma} k_{\min}^{\gamma-1} k_c^{n-(\gamma-1)} & \text{if } n > \gamma - 1. \end{cases} \quad (\text{B6})$$

Note that $\mu_n \sim \langle k^n \rangle$ is finite for $n < \gamma - 1$: in such a case, it is useful to have an explicit expression for μ_n , at least for $n = 1, 2, 3, 4$, those encountered in the main text. Using Eq. (A13) and [51] we get

$$\mu_1 = \langle k \rangle, \quad (\text{B7})$$

$$\mu_2 = \langle k^2 \rangle - \langle k \rangle, \quad (\text{B8})$$

$$\mu_3 = \langle k^3 \rangle - 3\langle k^2 \rangle + 2\langle k \rangle, \quad (\text{B9})$$

$$\mu_4 = \langle k^4 \rangle - 6\langle k^3 \rangle + 11\langle k^2 \rangle - 6\langle k \rangle. \quad (\text{B10})$$

For $n > \gamma - 1$ instead we have

$$\mu_n \simeq \frac{\gamma - 1}{n + 1 - \gamma} k_{\min}^{\gamma-1} k_c^{n-(\gamma-1)}. \quad (\text{B11})$$

Appendix C: High-order moments of P_K

From Eq. (1) and Eqs. (A8)-(A9), we can compute, at least in principle, every average with respect to P_K in \mathcal{G}_f , in terms of averages with respect to p_k . It is possible to obtain an explicit expression for $M_n = \langle K(K-1) \dots (K-n+1) \rangle = G_0^{(n)}(1)$ for arbitrary n using the Faà di Bruno's formula for the n -th derivative of a composite function [53]. Denoting with $D^n = (d/dz)^n$, we have

$$D^n [f(u(z))] = n! \sum_{m=1}^n \frac{f^{(m)}(u(z))}{m!} \sum_{i_1 + \dots + i_m = n} \prod_{j=1}^m \frac{u^{(i_j)}(z)}{i_j!}. \quad (\text{C1})$$

Writing $G_0(z) = g_0(\psi(z))$, where $\psi(z) = z g_1(1 - f + fz)$, it is easy to prove by induction that

$$\psi^{(n)}(z) = n f^{n-1} g_1^{(n-1)}(1 - f + fz) + f^n z g_1^{(n)}(1 - f + fz). \quad (\text{C2})$$

From Eq. (C1) with $f = g_0$ and $u = \psi$ evaluated at $z = 1$ we finally get, using Eqs. (A4)(A8),(C2)

$$M_n = n! \sum_{m=1}^n \frac{\mu_m}{m!} \sum_{s_1 + \dots + s_m = n} \prod_{j=1}^m \frac{[s_j f^{s_j-1} \mu_{s_j} + f^{s_j} \mu_{s_j+1}]}{\mu_1 s_j!}. \quad (\text{C3})$$

Eq. (C3) allows us to compute the expected number of $n - 1$ -stars and the generalized transitivity T_n for arbitrary $n > 1$ (see Sec. VB), but the computation becomes soon cumbersome. Nevertheless, with Eq. (C3) we can prove Eq.(23). In the case of PL backbones with $2 < \gamma < 3$, we have $\mu_j \sim k_c^{j+1-\gamma}$ for $j > 1$, while $\mu_1 \sim 1$, and $\psi^{(j)}(1) \sim f^j k_c^{j+2-\gamma}$ for $j \geq 1$. From Eq. (C3) we obtain

$$M_n \simeq a f^n k_c^{n+2-\gamma} + \sum_{m=2}^n b_m f^m k_c^{m+1-\gamma+m(3-\gamma)}, \quad (\text{C4})$$

where a, b_m are constants. The exponent $\alpha = m + 1 - \gamma + m(3 - \gamma)$ is a monotonically increasing function in m , hence its maximum value is reached for $m_\alpha = n$. Thus we have

$$M_n \simeq a f^n k_c^{n+2-\gamma} + b_n f^n k_c^{n+1-\gamma+n(3-\gamma)}. \quad (\text{C5})$$

The second term on the r.h.s. dominates for $2 < \gamma < 3 - 1/n$, while the first term dominates for $\gamma > 3 - 1/n$. For $\gamma > n + 2$, none of the terms appearing in Eq. (C3) diverges, hence $G_0^{(n)}(1) \sim 1$. Finally, for $3 - 1/n < \gamma < n + 2$ the leading term is always given by $k_c^{n+2-\gamma}$: some of the terms in the sum on the r.h.s. of Eq. (C4) $\psi^{s_j} \sim 1$, hence the exponent will be lower than α , and

since $\alpha < n + 2 - \gamma$ we can conclude that the leading order is given by the first term. With the substitution $n \rightarrow n - 1$ this yields Eq. (23).

Notice that for $3 < \gamma < 4$, since $M_n \sim \langle K^n \rangle$ and $\langle k^{n+1} \rangle \sim k_c^{n+1-\gamma}$, Eq. (C5) implies that, for $k_c \gg k_{\min}$, $\langle K^n \rangle \sim f^n \langle k^n \rangle$, as stated in Sec. VI.

-
- [1] P. Erdős and A. Rényi, On random graphs, *Publ. Math. Debrecen* **6**, 290 (1959).
- [2] P. Erdős and A. Rényi, On the evolution of random graphs, *Publ. Math. Inst. Hung. Acad. Sci.* **5**, 17 (1960).
- [3] B. Bollobás, A probabilistic proof of an asymptotic formula for the number of labelled regular graphs, *Eur. J. Comb.* **1**, 311 (1980).
- [4] M. Molloy and B. Reed, A critical point for random graphs with a given degree sequence, *Random Struct. Algorithms* **6**, 161 (1995).
- [5] M. E. J. Newman, S. H. Strogatz, and D. J. Watts, Random graphs with arbitrary degree distributions and their applications, *Phys. Rev. E* **64**, 026118 (2001).
- [6] S. N. Dorogovtsev and J. F. F. Mendes, *The Nature of Complex Networks* (Oxford University Press, 2022).
- [7] S. N. Dorogovtsev, A. V. Goltsev, and J. F. F. Mendes, Critical phenomena in complex networks, *Rev. Mod. Phys.* **80**, 1275 (2008).
- [8] R. Milo, S. Shen-Orr, S. Itzkovitz, N. Kashtan, D. Chklovskii, and U. Alon, Network motifs: simple building blocks of complex networks, *Science* **298**, 824 (2002).
- [9] M. A. Serrano and M. Boguñá, Percolation and epidemic thresholds in clustered networks, *Phys. Rev. Lett.* **97**, 088701 (2006).
- [10] M. A. Serrano and M. Boguñá, Clustering in complex networks. i. general formalism, *Phys. Rev. E* **74**, 056114 (2006).
- [11] M. A. Serrano and M. Boguñá, Clustering in complex networks. ii. percolation properties, *Phys. Rev. E* **74**, 056115 (2006).
- [12] D. Strauss, On a general class of models for interaction, *SIAM Rev.* **28**, 513 (1986).
- [13] T. A. Snijders, P. E. Pattison, G. L. Robins, and M. S. Handcock, New specifications for exponential random graph models, *Sociological methodology* **36**, 99 (2006).
- [14] G. Robins, P. Pattison, Y. Kalish, and D. Lusher, An introduction to exponential random graph (p^*) models for social networks, *Social Networks* **29**, 173 (2007).
- [15] G. Robins, T. Snijders, P. Wang, M. Handcock, and P. Pattison, Recent developments in exponential random graph (p^*) models for social networks, *Social Networks* **29**, 192 (2007).
- [16] F. Battiston, G. Cencetti, I. Iacopini, V. Latora, M. Lucas, A. Patania, J.-G. Young, and G. Petri, Networks beyond pairwise interactions: Structure and dynamics, *Physics Reports* **874**, 1 (2020).
- [17] J. Park and M. E. J. Newman, Solution for the properties of a clustered network, *Phys. Rev. E* **72**, 026136 (2005).
- [18] M. E. J. Newman, Properties of highly clustered networks, *Phys. Rev. E* **68**, 026121 (2003).
- [19] M. E. J. Newman, Random graphs with clustering, *Phys. Rev. Lett.* **103**, 058701 (2009).
- [20] J. C. Miller, Percolation and epidemics in random clustered networks, *Phys. Rev. E* **80**, 020901 (2009).
- [21] J. P. Gleeson, Bond percolation on a class of clustered random networks, *Phys. Rev. E* **80**, 036107 (2009).
- [22] B. Karrer and M. E. J. Newman, Random graphs containing arbitrary distributions of subgraphs, *Phys. Rev. E* **82**, 066118 (2010).
- [23] A. Rapoport, Spread of information through a population with socio-structural bias: I. assumption of transitivity, *The bulletin of mathematical biophysics* **15**, 523 (1953).
- [24] R. Toivonen, L. Kovanen, M. Kivelä, J.-P. Onnela, J. Saramäki, and K. Kaski, A comparative study of social network models: Network evolution models and nodal attribute models, *Social networks* **31**, 240 (2009).
- [25] T. A. Snijders, Statistical models for social networks, *Annual review of sociology* **37**, 131 (2011).
- [26] N. Z. Gong, W. Xu, L. Huang, P. Mittal, E. Stefanov, V. Sekar, and D. Song, Evolution of social-attribute networks: measurements, modeling, and implications using google+, in *Proceedings of the 2012 Internet Measurement Conference* (2012) p. 131.
- [27] P. Klimek and S. Thurner, Triadic closure dynamics drives scaling laws in social multiplex networks, *New Journal of Physics* **15**, 063008 (2013).
- [28] G. Bianconi, R. K. Darst, J. Iacovacci, and S. Fortunato, Triadic closure as a basic generating mechanism of communities in complex networks, *Physical Review E* **90**, 042806 (2014).
- [29] A. Asikainen, G. Iñiguez, J. Ureña-Carrión, K. Kaski, and M. Kivelä, Cumulative effects of triadic closure and homophily in social networks, *Science Advances* **6**, eaax7310 (2020).
- [30] T. P. Peixoto, Disentangling homophily, community structure, and triadic closure in networks, *Physical Review X* **12**, 011004 (2022).
- [31] P. Holme and B. J. Kim, Growing scale-free networks with tunable clustering, *Phys. Rev. E* **65**, 026107 (2002).
- [32] J. Davidsen, H. Ebel, and S. Bornholdt, Emergence of a small world from local interactions: Modeling acquaintance networks, *Phys. Rev. Lett.* **88**, 128701 (2002).
- [33] U. Bhat, P. L. Krapivsky, and S. Redner, Emergence of clustering in an acquaintance model without homophily, *Journal of Statistical Mechanics: Theory and Experiment* **2014**, 140101 (2014).
- [34] W. Levens, A. Szorkovszky, and D. J. T. Sumpter, Friend of a friend models of network growth, *Royal Society Open Science* **9**, 221200 (2022).
- [35] R. Zhang, D.-S. Lee, and C.-S. Chang, A generalized configuration model with triadic closure, *IEEE Transactions on Network Science and Engineering* **10**, 754 (2023).

- [36] L. Cirigliano, C. Castellano, and G. Timár, Extended-range percolation in complex networks, *Phys. Rev. E* **108**, 044304 (2023).
- [37] M. Catanzaro, M. Boguñá, and R. Pastor-Satorras, Generation of uncorrelated random scale-free networks, *Phys. Rev. E* **71**, 027103 (2005).
- [38] V. Latora, V. Nicosia, and G. Russo, *Complex Networks: Principles, Methods and Applications* (Cambridge University Press, 2017).
- [39] M. E. J. Newman, *Networks* (Oxford University Press, 2018).
- [40] G. Bianconi and M. Marsili, Loops of any size and hamilton cycles in random scale-free networks, *Journal of Statistical Mechanics: Theory and Experiment* **2005**, P06005 (2005).
- [41] R. van der Hofstad, J. S. van Leeuwen, and C. Stegehuis, Triadic closure in configuration models with unbounded degree fluctuations, *Journal of statistical physics* **173**, 746 (2018).
- [42] G. Timár, R. A. da Costa, S. N. Dorogovtsev, and J. F. F. Mendes, Approximating nonbacktracking centrality and localization phenomena in large networks, *Phys. Rev. E* **104**, 054306 (2021).
- [43] P. Colomer-de Simón, M. A. Serrano, M. G. Beiró, J. I. Alvarez-Hamelin, and M. Boguñá, Deciphering the global organization of clustering in real complex networks, *Scientific reports* **3**, 2517 (2013).
- [44] F. Chung, L. Lu, and V. Vu, Spectra of random graphs with given expected degrees, *Proc. Natl. Acad. Sci. USA* **100**, 6313 (2003).
- [45] C. Castellano and R. Pastor-Satorras, Relating topological determinants of complex networks to their spectral properties: Structural and dynamical effects, *Phys. Rev. X* **7**, 041024 (2017).
- [46] R. Pastor-Satorras and C. Castellano, Distinct types of eigenvector localization in networks, *Sci. Rep.* **6**, 18847 (2016).
- [47] H. S. Wilf, *generatingfunctionology* (CRC Press, 2005).
- [48] P. Flajolet and A. Odlyzko, Singularity analysis of generating functions, *SIAM J. Discret. Math.* **3**, 216 (1990).
- [49] D. J. Daley and D. Vere-Jones, *An Introduction to the Theory of Point Processes, Volume I: Elementary Theory and Methods* (Springer, 2003).
- [50] P. M. Knopf, The operator $(x \frac{d}{dx})^n$ and its applications to series, *Math. Mag.* **76**, 364 (2003).
- [51] D. E. Knuth, *The Art of Computer Programming, Volume 1 (3rd Edition)* (Addison Wesley Longman Publishing Co., Inc., USA, 1997).
- [52] T. M. Apostol, *Introduction to analytic number theory* (Springer Science & Business Media, 1998).
- [53] M. McKiernan, On the nth derivative of composite functions, *Am. Math. Mon.* **63**, 331 (1956).